Neurosci. Bull. June, 2019, 35(3):486–496
https://doi.org/10.1007/s12264-019-00338-z

www.neurosci.cn
www.springer.com/12264

ORIGINAL ARTICLE

MicroRNA-132 in the Adult Dentate Gyrus is Involved in Opioid Addiction *Via* Modifying the Differentiation of Neural Stem Cells

Meng Jia[1] · Xuewei Wang[1] · Haolin Zhang[1] · Can Ye[1] · Hui Ma[1] · Mingda Yang[1] · Yijing Li[1] · Cailian Cui[1]

Received: 24 April 2018 / Accepted: 10 October 2018 / Published online: 5 February 2019

Abstract MicroRNA-132 (miR-132), a small RNA that regulates gene expression, is known to promote neurogenesis in the embryonic nervous system and adult brain. Although exposure to psychoactive substances can increase miR-132 expression in cultured neural stem cells (NSCs) and the adult brain of rodents, little is known about its role in opioid addiction. So, we set out to determine the effect of miR-132 on differentiation of the NSCs and whether this effect is involved in opioid addiction using the rat morphine self-administration (MSA) model. We found that miR-132 overexpression enhanced the differentiation of NSCs *in vivo* and *in vitro*. Similarly, specific overexpression of miR-132 in NSCs of the adult hippocampal dentate gyrus (DG) during the acquisition stage of MSA potentiated morphine-seeking behavior. These findings indicate that miR-132 is involved in opioid addiction, probably by promoting the differentiation of NSCs in the adult DG.

Keywords miR-132 · Opioid addiction · Neural stem cell · Dentate gyrus

✉ Cailian Cui
clcui@bjmu.edu.cn

[1] Department of Neurobiology, School of Basic Medical Sciences, Key Laboratory for Neuroscience of the Ministry of Education and National Health and Family Planning Commission, Neuroscience Research Institute, Peking University, Beijing 100191, China

Introduction

MicroRNAs (miRs) are endogenous small (~22 nucleotides) noncoding RNAs that bind to the 3' untranslated region of target mRNAs to modulate the post-transcriptional regulation of gene expression *via* controlling the degradation and translation of mRNAs. The role of miRs in the central nervous system has been widely investigated, such as in neuronal development [1, 2], synapse formation, and plasticity [2, 3], and in the regulation of memory, cognition, and emotion [4–10].

miR-132 is considered to be a neural activity-regulating miR, the expression of which can be induced by transcription factor cAMP response element-binding protein [11]. Previous studies have shown that miR-132 is closely associated with neural plasticity, accelerating cell differentiation and synapse formation in embryonic neural stem cells (eNSCs) [12, 13] and increasing the complexity of dendrites and spine density of newborn neurons in the adult hippocampus of rodents [14, 15]. Adult neurogenesis includes proliferation and differentiation [16, 17]. The differentiation of NSCs involves their development into functional neurons and their linkage into existing neural circuits, so differentiation is far more closely associated with synaptic plasticity than proliferation [18, 19]. Intervention in differentiation is a more convenient and effective means of modulating neural plasticity.

Drug addiction is considered to be a brain disorder – a form of drug-induced neural plasticity [20] in which the expression of genes that are mainly related to neural plasticity and involved in learning, memory and motivational behaviors is altered by drug abuse [21]. miRNAs, regulators of the expression of these genes, have been shown to play critical roles in the development of drug addiction. For example, overexpression of miR-218

inhibits the heroin-induced reinstatement in both conditioned place preference and heroin self-administration [22]. It has been noted that the expression of miR-132 is induced after repeated morphine exposure, but the expression of miR-212 is downregulated in zebrafish embryos [23], suggesting that miR-132 but not miR-212 is closely associated with morphine addiction. However, recent work has mainly focused on the changes of expression after repeated morphine exposure, evidence on the changes of behavior induced by miR-132 is lacking.

Therefore, this study was designed to test whether miR-132 could influence the differentiation of NSC-like cells (Neuro 2A cells) and NSCs separated from embryos and further investigate the effect of miR-132 in NSCs of the adult dentate gyrus (DG) on morphine addiction using the rat morphine self-administration paradigm.

Materials and Methods

Animals

Adult male Sprague-Dawley rats weighing 320 g (8-weeks old) were housed under a 12-h reverse light/dark cycle (lights on at 19:00). The rats were adapted for 1 week before experimentation. All of the experimental procedures were in accordance with the National Institutes of Health Guide for the Care and Use of Laboratory Animals, and were approved by the Animal Use Committee of Peking University Health Science Center.

Cell Culture

Neuro 2A (N2a) cells were cultured in Dulbecco's modified Eagle's medium supplemented with 10% fetal bovine serum (HyClone, Logan, UT) at 37°C with 5% CO_2.

Sprague-Dawley rat neural stem cells (RASNF-01001, Cyagen, Guangzhou, China) were incubated in 5% CO_2 at 37°C. NSCs proliferated in rat neural stem cell basal medium (RASNF-90011, Cyagen) which contained 20 ng/mL epidermal growth factor (EGF) and 20 ng/mL basic fibroblast growth factor (bFGF). During the first 2 days of differentiation induction, the concentration of bFGF was decreased to 10 ng/mL. During the next 2 days, the concentrations of EGF and bFGF were decreased to 0 ng/mL and 5 ng/mL, respectively. During the last 2 days of differentiation induction, EGF and bFGF were omitted from the neural stem cell basal medium [24].

Vector Construction

The plasmid pCMV-MIR vector (OriGene, Rockville, MD) contained a cytomegalovirus (CMV) promoter, an miR-132 overexpression sequence (Gene ID: NR_031878.1) (defined as "miR-132 OE") or empty sequence (defined as "Control"), and an EGFP domain to label the transfected cells.

The lentivirus pLenti-CMV-mir-132 (OBiO, Shanghai, China) contained a CMV promoter, an miR-132 overexpression sequence (Gene ID: NR_031878.1) or empty sequence, and no EGFP.

The adeno-associated virus (AAV; OBiO) contained a nestin promoter which ensured that these AAVs were only expressed in NSCs, an miR-132 overexpression sequence (Gene ID: NR_031878.1) or empty sequence, and an EGFP domain.

The lentivirus system contained two lentiviruses: one with a nestin promoter and a reverse tetracycline-controlled transactivator (rtTA) element; the other with a tetracycline response (TRE) element, an EGFP element and an miR-132 overexpression sequence.

Cell Transfection

N2a cells were transfected with plasmid pCMV-MIR vector (Fig. 1A) to overexpress miR-132. N2a cells were passaged 24 h before transfection, and the plasmids were transfected into these cells with the transfection reagent Megatran 1.0 (OriGene), followed by morphological analysis 48 h later.

NSCs were transfected with pLenti-CMV-mir-132 using polybrene and harvested 48 h later.

Stereotactic Injection

Rats were bilaterally injected with the vectors in both the dorsal and ventral DG. The injection volume was 1 μL/site (AAV) or 0.5 μL/site (lentivirus). The viruses were slowly injected for 5 min and the injector was retained *in situ* for at least 2 min. The dorsal DG sites were 3.6 mm and 6.0 mm posterior to bregma, 2.2 mm and 5.2 mm from the midline, and 3.8 mm ventral from the pia mater. The ventral DG sites were 6.0 mm posterior to bregma, 5.2 mm from the midline, and 6.5 mm ventral from the pia mater.

Immunofluorescence

The N2a cells were washed three times with PBS, fixed in 4% paraformaldehyde (PFA) for 30 min at room

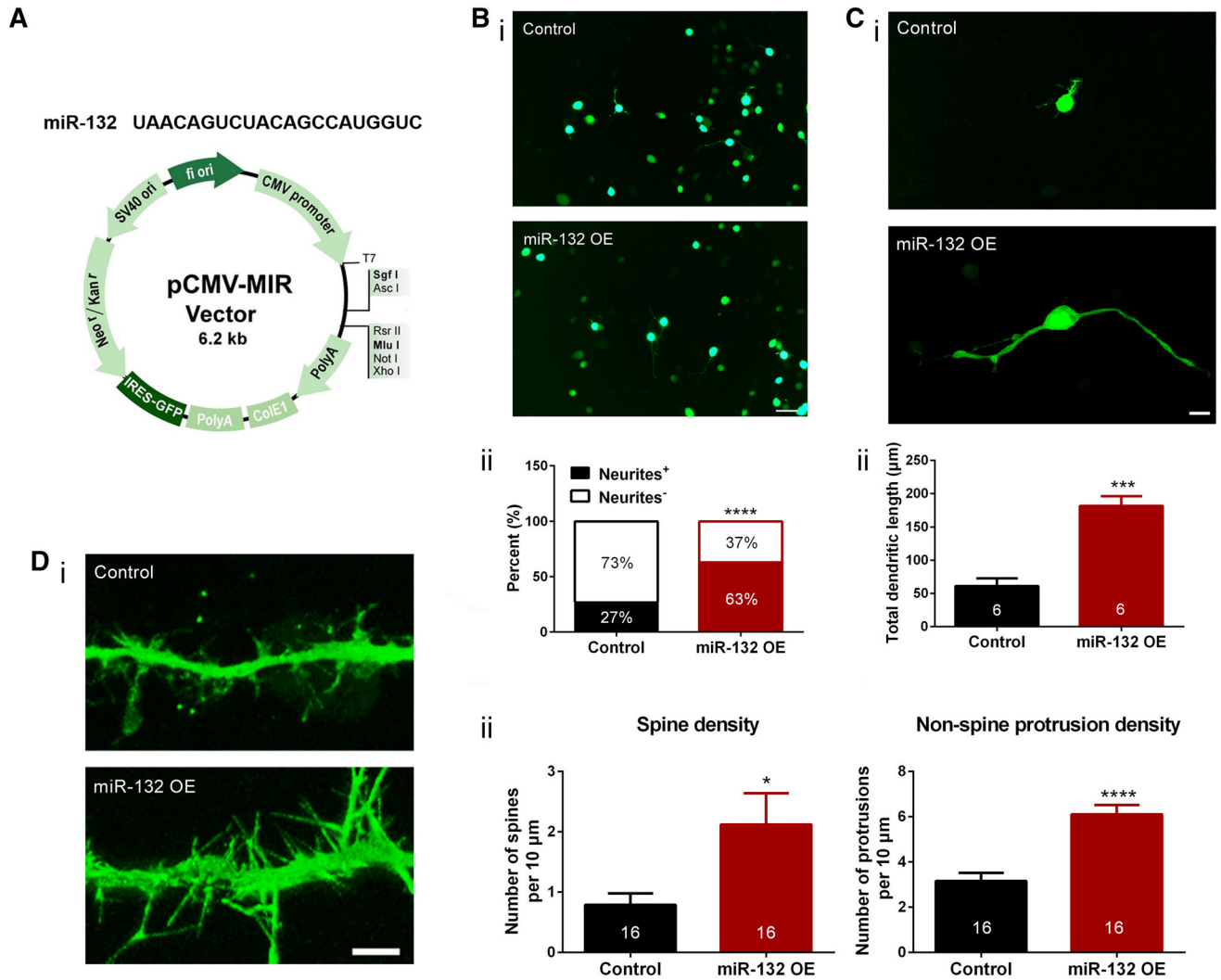

Fig. 1 Overexpression of miR-132 enhances neuronal differentiation of N2a cells. **A** Sequence of miR-132 and the structure of miR-132 overexpression plasmid. **B** Overexpression of miR-132 increased the percentage of cells with neurites. **i** Representative images of N2a cells after overexpression of miR-132. Scale bar, 50 μm. **ii** Overexpression of miR-132 resulted in neurite outgrowth in 63% of N2a cells, while control cells retained the neuroblastoma morphology. $****P < 0.0001$, χ^2 test. Data are shown as mean ± SEM. **C** Overexpression of miR-132 increases total dendritic length. **i** Representative images of N2a cells after overexpression of miR-132. Scale bar, 20 μm. **ii** Overexpression of miR-132 increased total dendritic length. $***P < 0.001$, unpaired Student's *t*-test. Data are shown as mean ± SEM. **D** Overexpression of miR-132 increased spine density. **i** Representative images of N2a cells after overexpression of miR-132. Scale bar, 5 μm. **ii** Overexpression of miR-132 increased dendritic spine and non-spine protrusion density. $*P < 0.05$, $****P < 0.0001$, unpaired Student's *t*-test. Data are shown as mean ± SEM.

temperature, washed three times with PBS, and screened under a confocal laser scanning microscope (FV1000, Olympus, Miyazaki, Japan). The percentages of neurites$^+$ and neurites$^-$ cells, as well as total dendritic length were determined manually under 400×, and the density of spine and non-spine protrusions was assessed under 3000×. A dendritic protrusion with an expanded head that was 50% wider than its neck was defined as a spine, and others were defined as non-spine protrusions [25]. The density was calculated from manual counts and normalized per 10 μm of dendritic length. Only dendrites with 50 μm or more of analyzable dendritic shaft were counted.

NSCs were washed and fixed as previously described. Then cells were incubated with blocking solution (5% donkey serum and 0.3% Triton X-100) for 1 h at room temperature to block nonspecific binding sites and permeabilize the membrane. The cells were incubated with primary antibody dilution buffer at 4°C overnight. On the next day, the cells were washed in PBS with 0.1% Tween 20 and incubated with secondary antibody dilution buffer containing Hoechst protected from light for 1 h at room temperature.

For brain sections, rats were perfused with 4% PFA and dehydrated for 7 days. Then the brains were quickly frozen

in liquid nitrogen and cut into coronal sections at 50 μm on a freezing microtome. Then the sections underwent the same procedure as for the NSCs.

Sholl and Total Dendritic Length Analysis

One section from each injection site in the DG was stained with Hoechst nuclear marker after virus injection. Three $EGFP^+$ neurons were randomly selected from each section and the images were collected in the form of collapsed z-stacks. The dendritic trees were reconstructed using the tracing tool of Adobe Illustrator CS5. Then, the complexity of dendritic trees was analyzed using the Sholl analyze plugin of ImageJ (NIH, Bethesda, MA) according to the procedure of Sholl Data Analysis [26].

The total dendritic length was defined as the summation of every branch of the dendrite and was also analyzed by ImageJ using the reconstructed image.

Flow Cytometry

NSCs were collected and incubated in Sprague-Dawley rat neural stem cell basal medium without EGF and bFGF but containing CD24 antibody protected from light for 25 min at 4°C. The cells were re-suspended gently at the mid-point of the incubation time. After washing in PBS with 5% fetal bovine serum (FBS), the cells were re-suspended in 1 mL 5% FBS and analyzed on a Caliber flow cytometer (BD Biosciences, San Jose, CA). Data were analyzed using FlowJo (Ashland, OR).

Real-Time qPCR

The miRNAs were extracted using TRIzol, then 3 μg miRNAs and 2 μL reverse transcription primer were used for reverse transcription. During the qPCR stage, the samples were mixed with 2 μL upstream primer and 2 μL downstream primer and each sample was replicated 3 times. The cycle conditions were: 3 s at 95°C, and 30 s at 60°C for 40 cycles, on the 7500 real-time system (Applied Biosystems). The data were standardized by glyceraldehyde-3-phosphate dehydrogenase. The relative fold change in expression of miR-132 was calculated using the comparative cycle threshold method ($2^{-\Delta\Delta CT}$). The primer sequences (synthetized by Sangon Biotech) are shown in Table 1.

Morphine Self-administration (MSA)

Rats were implanted with an intravenous catheter at the time of virus transfection, followed by 7 days of recovery. During the acquisition process, rats were given water containing doxycycline (dox) to overexpress miR-132, 3 h per day for 14 days under a fixed ratio 1 (FR1) pattern. The rats were allowed to freely explore a training box containing two nose-poke holes: one associated with the drug (active nose-pokes) with lights nearby, the other was the inactive hole without any lights. When the rats poked the active hole, they received an infusion and the light near the hole was turned down, accompanied by a cue light and a sound, followed by a 20-s no-reaction period. Rats received morphine at 125 μg/kg per infusion during the first 7 days, and the concentration of morphine was reduced to 67.5 μg/kg per infusion during the last 7 days. During the extinction process, rats were trained in the same context for 14 days without morphine injection and given normal water to stop the miR-132 overexpression.

Statistical Analyses

Student's *t*-test was used to compare parameters from two groups. The χ^2 test was used to analyze the percentage of cells with neurites. Two-way repeated measures ANOVA tests with Turkey's multiple comparison were used to analyze MSA behavior.

Results

Overexpression of miR-132 Enhances Neuronal Differentiation of N2a Cells

N2a cells are neuroblastoma cells that share properties with NSCs: (1) expression of the NSC marker nestin (from our

Table 1 The primer sequences.

Genes	Primers	Sequences (5′→3′)
GAPDH	RT primer	TGGCAAAGTGGAGATTGTT
	Upstream primer	CTTCTGGGTGGCAGTGAT
	Downstream primer	TGGCAAAGTGGAGATTGTT
miR-132	RT primer	GTCGTATCCAGTGCAGGGTCCGAGGTATTCGCA CTGGATACGACCGACCAT
	Upstream primer	CGCTAACAGTCTACAGCC
	Downstream primer	GCAGGGTCCGAGGTATTC

previous work); (2) self-renewal and differentiation into neuron-like cells; and (3) neurites and spine density become more complex with differentiation [27–31]. So, the N2a cell line is a suitable model for studying neural differentiation [28, 29, 31]. Forty-eight hours after transfection with pCMV-MIR, the percentage of N2a cells with neurites was significantly increased, 63% of the total cells in the miR-132 overexpression group grew neurites compared to 27% in the control group (Fig. 1B). The total dendritic length increased dramatically after overexpression of miR-132 (Fig. 1C), indicating that miR-132 extended the dendrites. Next, we calculated the spine density of N2a cells. According to the shape of the protrusions, they were divided into two categories - spines or non-spine protrusions. The short and mushroom-like protrusions with a slight neck and larger head were classified as spines, while long and sharp ones were classified as non-spine protrusions [25]. The density of both categories increased after miR-132 overexpression (Fig. 1D). All in all, overexpression of miR-132 pushed N2a cells towards differentiation, extended the dendrites, and enhanced the morphological development of dendrites.

Overexpression of miR-132 Increases Neuronal Differentiation of Cultured NSCs

Adult NSCs are widely believed to exist in the subgranular zone in the DG and the subventricular zone near the third ventricle, so we cultured NSCs separated from these two regions in rat embryos. To maintain the cells as stem cells, the growth medium contained high concentrations of EGF and bFGF (20 ng/mL). Nearly all the cultured cells expressed the NSC marker nestin, and a very small proportion expressed the neuronal precursor marker DCX, but they barely expressed the mature neuron marker NeuN or the glial marker GFAP (Fig. 2A). This kind of molecular marker expression pattern indicates that most of the cultured cells were NSCs, so they were used to study differentiation of NSCs according to Walker's protocol of cell proliferation and differentiation induction [24].

The lentivirus that overexpressed miR-132 was transfected on the 4th day of differentiation induction (Fig. 2B). The expression of miR-132 was significantly increased 48 h after lentivirus transfection (Fig. 2C). To reveal the morphology of NSCs, cells were labeled with the neuronal dendrite marker MAP2 and the nuclear stain Hoechst (Fig. 2D). Cells with tertiary branches were considered to have complex dendrites, and overexpression of miR-132 dramatically increased the percentage of cells with complex dendrites (Fig. 2E). Meanwhile, the total dendritic length also increased after miR-132 overexpression (Fig. 2E).

Then, we studied the percentage of well-differentiated cells by detecting a neural differentiation marker (CD24) on the membrane using flow cytometry [32]. Overexpression of miR-132 (Fig. 3A) significantly shifted the peak of CD24 expression histogram to the right (Fig. 3B), and the percentage of cells highly expressing CD24 was increased (Fig. 3C). In conclusion, miR-132 accelerates the differentiation of NSCs, especially the late stage of dendritic growth and arborization.

Overexpression of miR-132 Increases Neuronal Differentiation of NSCs in the DG

It is widely believed that the DG plays an important role in the formation and development of opioid addiction [33, 34]. So, apart from the evidence that miR-132 enhances the neuronal differentiation of NSCs *in vitro*, we also investigated the role of miR-132 in the differentiation of NSCs in the DG. We synthesized an AAV vector that contained a nestin promoter to specifically express this vector in NSCs, a miR-132 overexpression sequence, and an EGFP domain to label the infected NSCs (Fig. 4A). The injection sites of AAV into the DG are shown in Fig. 4B. The viruses were transfected 7 days before the differentiation stage to ensure full expression, and then another 14 days were allowed to elapse to match the 14-day self-administration training phase (Fig. 4C). Sholl analysis [26] showed that overexpression of miR-132 significantly increased the complexity of the dendritic tree and the total dendritic length of newborn neurons (Fig. 4D). These results indicate that specifically overexpressing miR-132 in NSCs in the adult DG enhances the differentiation of NSCs in the DG.

Specifically Overexpressing miR-132 in the NSCs of the Adult DG Potentiates MSA

To investigate whether the enhanced differentiation of NSCs in the DG induced by miR-132 can affect morphine-seeking behavior, we designed a time-specific expression lentivirus system to overexpress miR-132 under the control of dox. This system contained two lentiviruses, one with an rtTA element that bound to dox and was activated by it, and the other with a TRE element, the expression of which was regulated by rtTA, followed by an EGFP element and the miR-132 overexpression sequence or nothing. Thus, when dox was present, the rtTA was turned on and miR-132 began to be overexpressed (Fig. 5A). The EGFP represented miR-132, specifically merged with nestin but not NeuN, and lasted for at least 28 days until these cells developed into mature neurons (Fig. 5B). These lentiviruses had been synthesized and verified in our previous work [Haolin Zhang *et al.*, accepted by Scientific Reports].

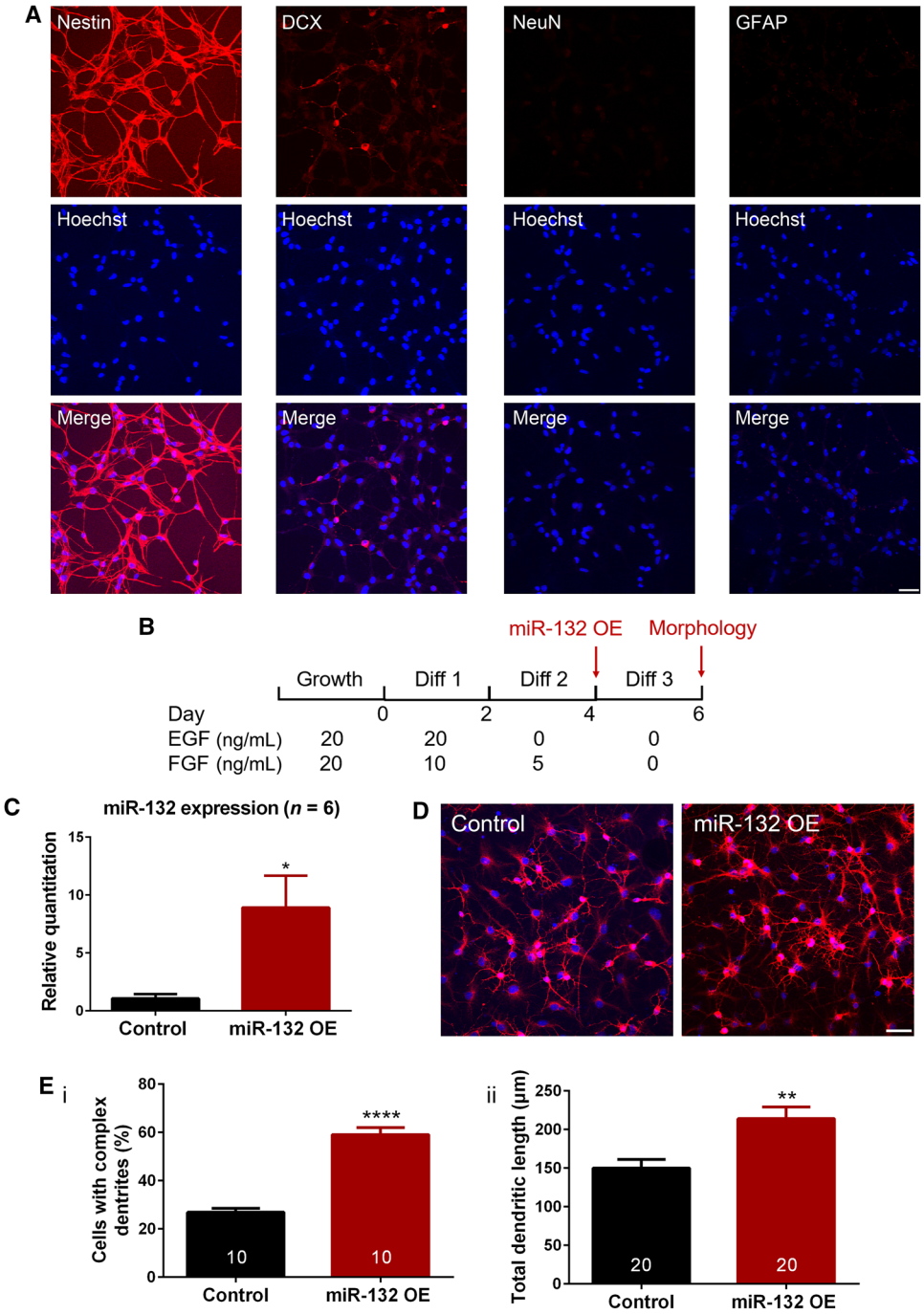

Fig. 2 Overexpression of miR-132 increases neuronal differentiation of cultured NSCs. **A** Cultured NSCs strongly expressed the NSC marker nestin, weakly expressed the neuronal precursor marker DCX, but barely expressed the neuronal marker NeuN and glial marker GFAP. Scale bar, 20 μm. **B** Schematic diagram outlining the procedure for inducing the differentiation of cultured NSCs. **C** The miR-132 overexpression lentivirus induced the expression of miR-132. **D** Representative images of cell morphology of NSCs after overexpression of miR-132. Cells were labeled by the neuronal differentiation marker MAP2 (red) and the nuclear stain Hoechst (blue). Scale bar, 20 μm. **E** Overexpression of miR-132 advanced the differentiation of cultured NSCs. **i** Overexpression of miR-132 increased the percentage of cells with complex dendrites. **ii** Overexpression of miR-132 increased the total dendritic length. $^{*}P < 0.05$, $^{**}P < 0.01$, $^{****}P < 0.0001$; unpaired Student's *t*-test. Data are shown as mean ± SEM.

miR-132 was conditionally overexpressed in the DG of adult rats during MSA training and stopped at the beginning of MSA extinction (Fig. 5C). During the training stage, rats in the group overexpressing miR-132 received notably more infusions than rats in the control group, and the infusions increased after the concentration of morphine

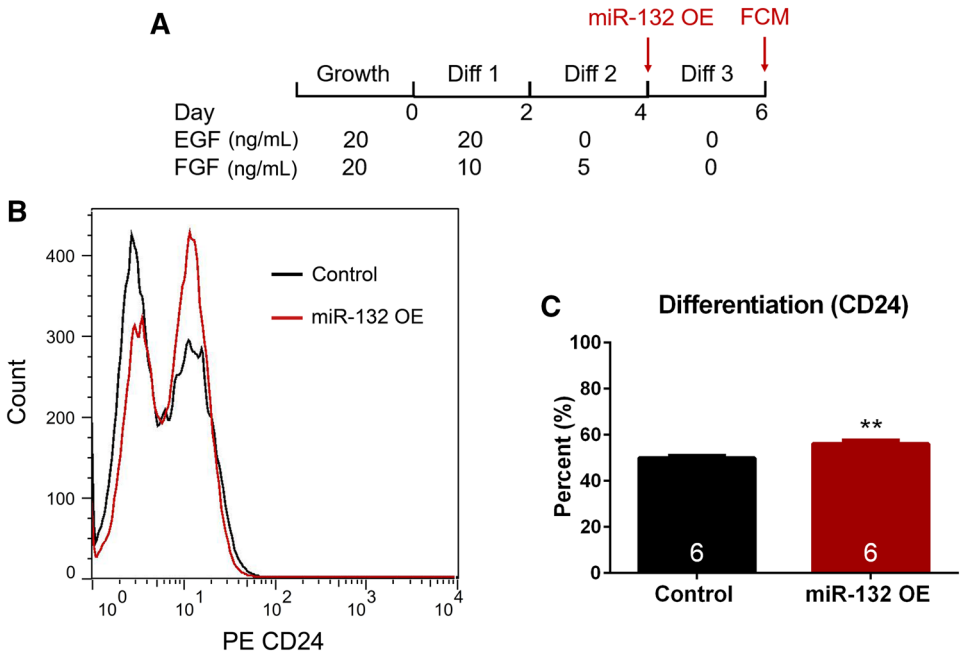

Fig. 3 Overexpression of miR-132 increases the percentage of well-differentiated cells. **A** Schematic diagram outlining the procedure of inducing differentiation of cultured NSCs. **B** Representative flow cytometry image of P-phycoerythrin (PE) CD24. **C** Quantification of differentiation using fluorescence intensity. $^{**}P < 0.01$, unpaired Student's *t*-test. Data are shown as mean ± SEM.

was reduced to 62.5 μg/kg per infusion (Fig. 5Di). Meanwhile, these two groups had similar numbers of inactive nose-pokes (Fig. 5Dii). The data from the first 7 days and the next 7 days were analyzed separately. miR-132 overexpression only increased the number of infusions during the next 7 days but not the first 7 days (Fig. 5Diii). During the extinction stage, although the numbers of mock infusions in these two groups showed no significant differences, the group overexpressing miR-132 had more mock infusions (Fig. 5Ei). Numbers of inactive nose-pokes also remained in balance (Fig. 5Eii). To reduce individual differences in sensitivity to morphine among the rats, we introduced an extinction trend curve (ETC) in which the mock infusions of rats on each day were normalized by their own mock infusions on the 1st day, so that each rat started the extinction process at the same level. Rats in the group overexpressing miR-132 showed a significant rise of ETC that was maintained at a high level (> 1) for at least 10 days, whereas the ETC of the control group decreased gradually and was maintained at a lower level than on the 1st day (Fig. 5Eiii). These findings indicate that overexpressing miR-132 specifically in the NSCs of the adult DG accompanied by MSA training accelerates the acquisition and resists the extinction of MSA even when the overexpression is stopped.

Discussion

In this work we found that overexpression of miR-132 *in vitro* enhanced the differentiation of NSC-like cells (N2a cells) and NSCs. *In vivo*, specific overexpression of miR-132 in the NSCs of the adult DG in rats enhanced their differentiation. Furthermore, specific overexpression of miR-132 in the NSCs of the adult DG during the training stage of MSA accelerated the acquisition and resisted the extinction of MSA. These findings indicate that miR-132 in the adult DG is involved in modulating opioid addiction *via* enhancing the differentiation of local NSCs.

We found that miR-132 overexpression enhanced the differentiation of not only cultured NSCs *in vitro* but also the NSCs in the adult DG *in vivo*. These results are consistent with previous studies. Yoshimura *et al.* reported that miR-132 expression increases in the neuronal development stage of embryos (E16.5 to E19.5), especially in extension of the axons of developing neurons [12, 13] and miR-132 mimics significantly lengthen axons, but miR-132 inhibition has the opposite effect [13]. In addition, miR-132 is known to regulate the differentiation of newborn and mature neurons in the hippocampus, that the inhibition or knockdown of miR-132 suppresses dendritic morphogenesis and decreases the spine density of newborn neurons, and miR-132 overexpression increases the spine density of mature neurons in the hippocampus [10, 14, 15].

Apart from the effect on morphological plasticity, miR-132 has also been shown to modulate the functional plasticity of neurons – both spontaneous [14, 35, 36] and evoked [37] synaptic transmission. Pathania *et al.* showed that the mean amplitude and frequency of spontaneous excitatory postsynaptic currents are decreased after miR-132 inhibition [14]. Further, Lambert *et al.* showed that miR-132 overexpression increases the paired-pulse ratio and decreases synaptic depression in primary hippocampal neurons [37].

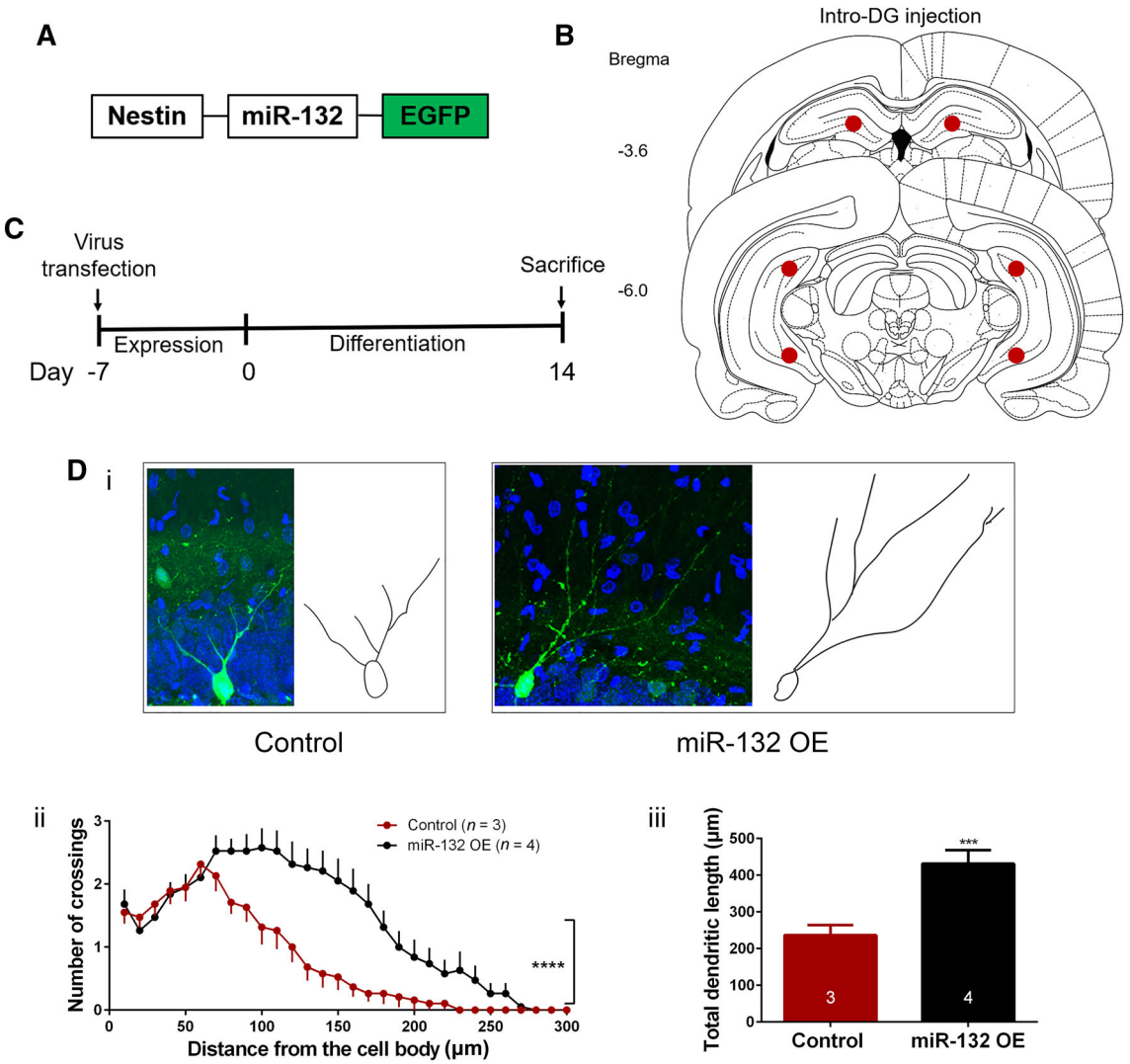

Fig. 4 Overexpression of miR-132 promotes the differentiation of NSCs in the adult DG. **A** Schematic image of the AAV vector construct designed to overexpress miR-132. **B** Infection sites in the dorsal and ventral DG. **C** Schematic of experimental procedures. **D** Specific overexpression of miR-132 in NSCs in the adult DG promotes neuronal differentiation. **i** Representative images and their reconstruction. **ii** Quantification of the complexity of dendritic trees. $^{****}P < 0.0001$; two-way repeated measures ANOVA. **iii** Quantification of total dendritic length, $^{***}P < 0.001$; unpaired Student's *t*-test. Data are shown as mean ± SEM.

Drug addiction is thought to be a form of pathological memory and drug-induced neural plasticity. Neural plasticity of the hippocampus is believed to be involved in pattern-separation behavioral tasks that involve spatial and context recognition memory [38]. Saxe *et al.* found that preventing neurogenesis in the DG impairs the induction of long-term potentiation and contextual fear conditioning but not cued fear conditioning [39], indicating that neural plasticity in the hippocampus plays an important role in context recognition memory tasks. Since miR-132 modulates morphological and functional plasticity, it acts as a regulator of memories. For example, Hansen *et al.* reported that miR-132 overexpression enhances spatial memory. However, these studies mostly controlled the expression of miR-132 (either overexpression or knockdown) in nearly all neurons or the excitatory neurons ($CaMII^{+}$) in the regions of interest, and there is no evidence on the role of miR-132 in drug-associated contextual memory tasks. So, we specifically overexpressed miR-132 in the NSCs ($nestin^{+}$ cells) in the adult DG in a time-specific manner during the training process and found that this potentiated the acquisition and resisted the extinction of MSA. Interestingly, studies on the regulation of miR-132 expression indicate that the miR-132 expression after repeated morphine exposure is ~1.3-fold that of the group without morphine exposure [23]. Hansen and colleagues found a 1.5-fold increase in the expression of miR-132 within CA1, CA3, and the DG after a spatial memory task, which is

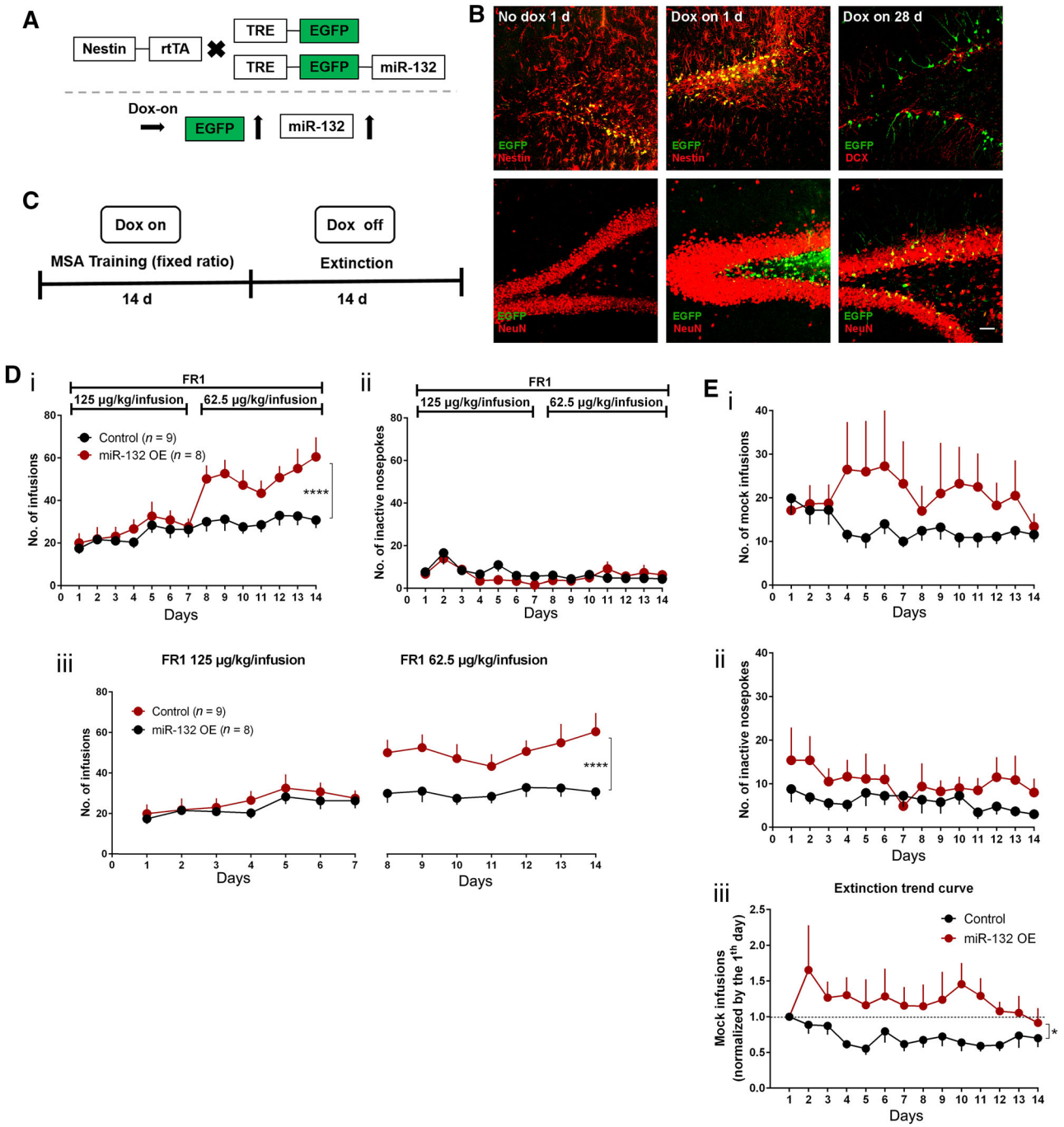

Fig. 5 Overexpression of miR-132 in the NSCs of the adult DG of rats potentiates morphine self-administration. **A** Schematic of the lentivirus construct designed to overexpress miR-132. **B** Left and middle panels: EGFP was only expressed in nestin$^+$ cells. Right panels: EGFP$^+$ cells were NeuN$^+$ and not DCX$^+$ 28 days after transfection. Scale bar, 50 μm. **C** Schematic of experimental procedures. **D** Training process for morphine self-administration. **i** NSC-specific miR-132 overexpression increases morphine intake during the acquisition phase. **ii** Rats overexpressing miR-132 and controls nose-poked the inactive hole at similar rates. **iii** miR-132 overexpression increased the injections during the next 7 days but not the first 7 days. **E** The extinction process of morphine self-administration. **i** Control and miR-132 rats in the absence of dox showed comparable drug-seeking behavior during extinction. **ii** miR-132 rats without dox showed more inactive nose-pokes than control rats during extinction. **iii** Control rats showed a slowly declining curve, yet rats overexpressing miR-132 maintained a high level of normalized mock infusions. Genotype × Day: $^*P < 0.05$, $^{****}P < 0.0001$; two-way repeated measures ANOVA. Data are shown as mean ± SEM.

similar to the miR-132 increase induced by morphine exposure. Then, they introduced regulatable overexpression of miR-132 (< 2-fold) increase of miR-132 overexpression enhanced spatial memory, while a high level of overexpression (> 3-fold) had the opposite effect [10, 40]. The effective memory enhancement of miR-132 coincides with the changed level of miR-132 expression after a spatial memory task as well as morphine exposure, indicating that spatial memory shares a neural plasticity mechanism with morphine addiction memory – enhanced neural differentiation. However, although we showed that overexpression of miR-132 in the NSCs of the adult DG potentiates drug-seeking behavior, morphological evidence of NSCs in the adult DG after miR-132 overexpression is needed in further studies.

In this research, we first found that specific overexpression of miR-132 in the NSCs of the adult DG accelerates the acquisition of MSA, represented by the increased number of infusions, indicating that miR-132 potentiates morphine-seeking. Further analysis showed that miR-132 only increased the number of infusions during the next 7 days, but not the first 7 days of MSA training. First, the increased number of infusions (active nose-pokes) responding to the half-dose of morphine revealed "reliably acquired drug self-administration" [41–44], so the effect of miR-132 overexpression during the next 7 days of MSA reflected the true effect on the acquisition of MSA. Second, the number of infusions of heroin self-administration doubled after the dose was halved [45, 46]. However, in MSA, although the number of infusions also increased after halving the dose, the increase did not reach 2-fold. This revealed that sensitivity of rats to morphine is not as high as to heroin, but miR-132 overexpression specifically increases the number of infusions after halving the dose of morphine, indicating that miR-132 increases the sensitivity to morphine. Third, in MSA the rewarding effect has an associated memory; when the dose of morphine is halved, the rats need more injections to achieve an equal rewarding effect. This means that the stronger the memory of a prior reward, the more injections needed to satisfy the drug-seeking motivation evoked by drug-related context memory. So, the enhancement of the acquisition of MSA by miR-132 is probably through strengthening the memory associated with the drug-reward, and this is consistent with the finding that miR-132 enhances hippocampus-associated memories *via* modulating the differentiation of NSCs.

During the extinction process, the number of mock infusions in the control group rapidly dropped to 10 on the 4th day and maintained this level until the 14th day. As to the group overexpressing miR-132, the number of mock infusions remained at a higher level for several days, and then slowly decreased to 10 on the 14th day. Although these two curves have no remarkable statistical difference, the differences between the two groups might be hidden by the individual differences among rats. To minimize these individual differences, we introduce the ETC which may reflect the extinction trend. The ETC of the group overexpressing miR-132 was significantly different from the control group, which is always > 1 during the 14 extinction days, yet the ETC of the control group gradually declined. These results strongly suggest that overexpression of miR-132 in the NSCs of the adult DG enhances the consolidation and impairs the elimination of addiction memory.

Acknowledgements This work was supported by grants from the National Natural Science Foundation (81471353 and 81771433), the National Basic Research Development Program of China (2015CB553500), and the Science Fund for Creative Research Groups from the National Natural Science Foundation of China (81521063).

Conflict of interest The authors declare no competing interests.

References

1. Pandey A, Singh P, Jauhari A, Singh T, Khan F, Pant AB, *et al.* Critical role of the miR-200 family in regulating differentiation and proliferation of neurons. J Neurochem 2015, 133: 640–652.
2. Sim SE, Bakes J, Kaang BK. Neuronal activity-dependent regulation of microRNAs. Mol Cell 2014, 37: 511–517.
3. Ashraf SI, Mcloon AL, Sclarsic SM, Kunes S. Synaptic protein synthesis associated with memory is regulated by the RISC pathway in *Drosophila*. Cell 2006, 124: 191–205.
4. Wei CW, Luo T, Zou SS, Wu AS. Research progress on the roles of microRNAs in governing synaptic plasticity, learning and memory. Life Sci 2017, 188: 118–122.
5. Nadim WD, Simion V, Benedetti H, Pichon C, Baril P, Morissetlopez S. MicroRNAs in neurocognitive dysfunctions: new molecular targets for pharmacological treatments? Curr Neuropharmacol 2017, 15: 260–275.
6. Zhang T, Zhao X, Steer CJ, Yan G, Song G. A negative feedback loop between microRNA-378 and Nrf1 promotes the development of hepatosteatosis in mice treated with a high fat diet. Metabolism 2018, 85: 183–191.
7. Mathew RS, Tatarakis A, Rudenko A, Johnsonvenkatesh EM, Yang YJ, Murphy EA, *et al.* A microRNA negative feedback loop downregulates vesicle transport and inhibits fear memory. eLife 2016, 5. pii: e22467.
8. Scott HL, Tamagnini F, Narduzzo KE, Howarth JL, Lee YB, Wong LF, *et al.* MicroRNA-132 regulates recognition memory and synaptic plasticity in the perirhinal cortex. Eur J Neurosci 2012, 36: 2941–2948.
9. Aten S, Hansen KF, Hoyt KR, Obrietan K. The miR-132/212 locus: a complex regulator of neuronal plasticity, gene expression and cognition. RNA Dis 2016, 3. pii: e1375.
10. Hansen KF, Sakamoto K, Wayman GA, Impey S, Obrietan K. Transgenic miR132 alters neuronal spine density and impairs novel object recognition memory. PLoS One 2010, 5: e15497.
11. Nudelman AS, Dirocco DP, Lambert TJ, Garelick MG, Le J, Nathanson NM, *et al.* Neuronal activity rapidly induces transcription of the CREB-regulated microRNA-132, *in vivo*. Hippocampus 2010, 20: 492–498.

12. Yoshimura A, Numakawa T, Odaka H, Adachi N, Tamai Y, Kunugi H. Negative regulation of microRNA-132 in expression of synaptic proteins in neuronal differentiation of embryonic neural stem cells. Neurochem Int 2016, 97: 26–33.
13. Hancock ML, Preitner N, Quan J, Flanagan JG. MicroRNA-132 is enriched in developing axons, locally regulates Rasa1 mRNA, and promotes axon extension. J Neurosci 2014, 34: 66–78.
14. Pathania M, Torres-Reveron J, Yan L, Kimura T, Lin TV, Gordon V, *et al.* miR-132 enhances dendritic morphogenesis, spine density, synaptic integration, and survival of newborn olfactory bulb neurons. PLoS One 2012, 7: e38174.
15. Magill ST, Cambronne XA, Luikart BW, Lioy DT, Leighton BH, Westbrook GL, *et al.* microRNA-132 regulates dendritic growth and arborization of newborn neurons in the adult hippocampus. Proc Natl Acad Sci U S A 2010, 107: 20382–20387.
16. Ming GL, Song H. Adult neurogenesis in the mammalian brain: significant answers and significant questions. Neuron 2011, 70: 687–702.
17. Gould E. How widespread is adult neurogenesis in mammals? Nat Rev Neurosci 2007, 8: 481–488.
18. Luikart BW, Perederiy JV, Westbrook GL. Dentate gyrus neurogenesis, integration and microRNAs. Behav Brain Res 2012, 227: 348–355.
19. Tashiro A, Sandler VM, Toni N, Zhao C, Gage FH. NMDA-receptor-mediated, cell-specific integration of new neurons in adult dentate gyrus. Nature 2006, 442: 929–933.
20. Nestler EJ, Hope BT, Widnell KL. Drug addiction: a model for the molecular basis of neural plasticity. Neuron 1993, 11: 995–1006.
21. Nestler EJ. Molecular basis of long-term plasticity underlying addiction. Nat Rev Neurosci 2001, 2: 119–128.
22. Yan B, Hu Z, Yao W, Le Q, Bo X, Xing L, *et al.* MiR-218 targets MeCP2 and inhibits heroin seeking behavior. Sci Rep 2017, 7: 40413.
23. Jimenezgonzalez A, Garcíaconcejo A, Lópezbenito S, Gonzaleznunez V, Arévalo JC, Rodriguez RE. Role of morphine, miR-212/132 and mu opioid receptor in the regulation of bdnf in zebrafish embryos. Biochim Biophys Acta 2016, 1860: 1308–1316.
24. Walker TL, Kempermann G. One mouse, two cultures: isolation and culture of adult neural stem cells from the two neurogenic zones of individual mice. J Vis Exp 2014, 84: e51225.
25. Miller EC, Zhang L, Dummer BW, Cariveau DR, Loh H, Law PY, *et al.* Differential modulation of drug-induced structural and functional plasticity of dendritic spines. Mol Pharmacol 2012, 82: 333.
26. Sholl DA. Dendritic organization in the neurons of the visual and motor cortices of the cat. J Anat 1953, 87: 387–406.
27. Sidiropoulou E, Sachana M, Flaskos J, Harris W, Hargreaves AJ, Woldehiwet Z. Fipronil interferes with the differentiation of mouse N2a neuroblastoma cells. Toxicol Lett 2011, 201: 86–91.
28. Tremblay RG, Sikorska M, Sandhu JK, Lanthier P, Ribecco-Lutkiewicz M, Bani-Yaghoub M. Differentiation of mouse Neuro 2A cells into dopamine neurons. J Neurosci Methods 2010, 186: 60–67.
29. Wu G, Fang Y, Lu ZH, Ledeen RW. Induction of axon-like and dendrite-like processes in neuroblastoma cells. J Neurocytol 1998, 27: 1–14.
30. Dickey CA, De Mesquita DD, Morgan D, Pennypacker KR. Induction of memory-associated immediate early genes by nerve growth factor in rat primary cortical neurons and differentiated mouse Neuro2A cells. Neurosci Lett 2004, 366: 10–14.
31. Saragoni L, Hernández P, Maccioni RB. Differential association of tau with subsets of microtubules containing posttranslationally-modified tubulin variants in neuroblastoma cells. Neurochem Res 2000, 25: 59–70.
32. Pastrana E, Cheng LC, Doetsch F. Simultaneous prospective purification of adult subventricular zone neural stem cells and their progeny. Proc Natl Acad Sci U S A 2009, 106: 6387–6392.
33. Yue Z, Loh HH, Ping-Yee L. Effect of opioid on adult hippocampal neurogenesis. ScientificWorldJournal 2016, 2016: 2601264.
34. Kang E, Wen Z, Song H, Christian KM, Ming GL. Adult neurogenesis and psychiatric disorders. Cold Spring Harb Perspect Biol 2016, 8: a019026.
35. Impey S, Davare M, Lesiak A, Lasiek A, Fortin D, Ando H, *et al.* An activity-induced microRNA controls dendritic spine formation by regulating Rac1-PAK signaling. Mol Cell Neurosci 2010, 43: 146–156.
36. Luikart BW, Bensen ASL, Washburn EK, Perederiy JV, Su KG, Li Y, *et al.* miR-132 mediates the integration of newborn neurons into the adult dentate gyrus. PLoS One 2011, 6: e19077.
37. Lambert TJ, Storm DR, Sullivan JM. MicroRNA132 modulates short-term synaptic plasticity but not basal release probability in hippocampal neurons. PLoS One 2016, 5: e15182.
38. Gonçalves JT, Schafer ST, Gage FH. Adult neurogenesis in the hippocampus: from stem cells to behavior. Cell 2016, 167: 897–914.
39. Saxe MD, Battaglia F, Wang JW, Malleret G, David DJ, Monckton JE, *et al.* Ablation of hippocampal neurogenesis impairs contextual fear conditioning and synaptic plasticity in the dentate gyrus. Proc Natl Acad Sci U S A 2006, 103: 17501–17506.
40. Hansen KF, Karelina K, Sakamoto K, Wayman GA, Impey S, Obrietan K. miRNA-132: a dynamic regulator of cognitive capacity. Brain Struct Funct 2013, 218: 817–831.
41. Bossert JM, Gray SM, Lu L, Shaham Y. Activation of group II metabotropic glutamate receptors in the nucleus accumbens shell attenuates context-induced relapse to heroin seeking. Neuropsychopharmacology 2006, 31: 2197–2209.
42. Yokel RA. Intravenous self-administration: response rates, the effects of pharmacological challenges, and drug preference. In: Bozarth MA (Ed.). Methods of Assessing the Reinforcing Properties of Abused Drugs. New York: Springer, 1987.
43. Shaham Y, Erb S, Stewart J. Stress-induced relapse to heroin and cocaine seeking in rats: a review. Brain Rese Rev 2000, 33: 13–33.
44. Bossert JM, Liu SY, Lu L, Shaham Y. A role of ventral tegmental area glutamate in contextual cue-induced relapse to heroin seeking. J Neurosci 2004, 24: 10726.
45. Ge F, Wang N, Cui C, Li Y, Liu Y, Ma Y, *et al.* Glutamatergic projections from the entorhinal cortex to dorsal dentate gyrus mediate context-induced reinstatement of heroin seeking. Neuropsychopharmacology 2017, 42: 1860.
46. Wang N, Ge F, Cui C, Li Y, Sun X, Sun L, *et al.* Role of glutamatergic projections from the ventral CA1 to infralimbic cortex in context-induced reinstatement of heroin seeking. Neuropsychopharmacology 2018, 43: 1373–1384.